Research Square

Preprints are preliminary reports that have not undergone peer review.
They should not be considered conclusive, used to inform clinical practice,
or referenced by the media as validated information.

Extension of unstable dissipative systems to the fractional-order case with applications in the design of multi-scroll attractors

María A. Mata-González
Instituto Tecnológico de Tijuana
Jesus R. Pulido–Luna
CICESE
Joaquín Álvarez
CICESE
Jorge A. López–Rentería
jorge.lopez@tectijuana.edu.mx

Secretaría de Ciencia, Humanidades, Tecnología e Innovación

Research Article

Keywords: Fractional-order systems, Unstable dissipative systems, Signed distance function, Matignon stability criterion, Piecewise-linear systems, Multi-scroll attractors

Posted Date: November 9th, 2026

DOI: https://doi.org/10.21203/rs.3.rs-11641427/v1

License: This work is licensed under a Creative Commons Attribution 4.0 International License.
Read Full License

Additional Declarations: No competing interests reported.

Extension of unstable dissipative systems to the fractional-order case with applications in the design of multi-scroll attractors

María A. Mata–González[1,2†], Jesus R. Pulido–Luna[3,4†], Joaquín Álvarez[3], Jorge A. López–Rentería[1,5*]

[1*]Departamento de Ingeniería Eléctrica y Electrónica, Tecnológico Nacional de México / Instituto Tecnológico de Tijuana, Calzada Tecnológico No. 12950, Tijuana, 22414, Baja California, México.
[2]CETYS Universidad, Av. CETYS Universidad No. 4, Tijuana, 22217, Baja California, México.
[3]Departamento de Electrónica y Telecomunicaciones, CICESE, Carretera Ensenada - Tijuana No. 3918, Ensenada, 22860, Baja California, México.
[4]Departamento de Investigación y Posgrado, Universidad Tecnológica de Tijuana, Carretera Libre Tijuana-Tecate Km. 10, Tijuana, 22253, Baja California, México.
[5*]Investigadoras e Investigadores por México, Secihti, Av. Insurgentes Sur 1582, Demarcación Territorial Benito Juárez, 03940, Ciudad de México, México.

*Corresponding author(s). E-mail(s): jorge.lopez@tectijuana.edu.mx;
Contributing authors: m25210053@tectijuana.edu.mx, angeles.mata@cetys.mx; jpulido@cicese.edu.mx, jesus.pulido@uttijuana.edu.mx; jqalvar@cicese.edu.mx;
†These authors contributed equally to this work.

Abstract

Piecewise-linear unstable dissipative systems (UDS's) are a class of dynamical systems that are able to generate multi-scroll attractors through the spectral properties of their equilibria. The goal of this work is to extend the UDS's to the fractional-order case. To achieve it, a distance to the boundary of the fractional stability region is proosed in terms of the signed distance definition. The resulting

definition covers both types of unstable dissipative systems and recovers the classical one in the integer-order case. For a given system, it also gives the range of fractional orders in which the system belongs to each type. The definition is applied to the design of two piecewise-linear systems that generate single-scroll and multi-scroll attractors.

Keywords: Fractional-order systems, Unstable dissipative systems, Signed distance function, Matignon stability criterion, Piecewise-linear systems, Multi-scroll attractors

MSC Classification: 34A08 , 26A33 , 34A36 , 34D20 , 34C28

1 Introduction

Chaotic behavior has been studied extensively because of its applications in science and engineering. Although there is no unified definition of chaos, sensitivity to initial conditions and density of periodic orbits are common properties of chaotic systems [1]. The Rössler and Duffing oscillators, the Lorenz-type systems (Lorenz, Lü and Chen systems), among others, are perhaps the most studied objects in dynamical systems that exhibit this class of complex solutions in continuous or discrete time [1–4].

A particular class of systems, studied in [5, 6], is defined in $\mathbb{R}^3$, the lowest dimension where chaotic behavior is exhibited. These systems are the so-called *unstable dissipative systems* (UDS), whose complex dynamics are governed by the spectral properties of their equilibria. That is, the equilibrium points are saddle-focus (possessing a pair of complex conjugate eigenvalues and one real eigenvalue) satisfying the dissipative condition, which requires the sum of the eigenvalues to be negative. There are two types of UDS: type I possesses a stable manifold of dimension two, generated by the eigenvectors associated with the pair of complex conjugate eigenvalues with negative real part, and an unstable manifold of dimension one, associated with the positive real eigenvalue. Type II is composed of an unstable manifold of dimension two, generated by the eigenvectors associated with the pair of complex conjugate eigenvalues with positive real part, and a stable manifold of dimension one, associated with the negative real eigenvalue.

Unstable dissipative systems whose nonlinearity is constructed using piecewise-linear systems have been studied in several works, where they generate chaotic behavior in the form of multi-scroll attractors [5–10]. The design of UDS using piecewise-linear systems has been further extended to fractional-order systems in order to achieve chaotic behavior [11]. Although many definitions of the fractional integro-derivative exist, the most widely used are the Riemann–Liouville, Caputo, and Grünwald–Letnikov definitions [12–20]. Among their applications, chaotic systems are used in secure communications, where synchronization and the generation of pseudo-random bits allow information to be encrypted and decrypted by two parties that know the system, which is the shared key [9, 21, 22]. The implementation of electronic circuits in chaotic systems has also been explored [23–26]. Unstable dissipative systems of integer and fractional order with this kind of complex behavior have been designed in [5–10, 27–30].

The aim of this work is to formalize the definition of unstable dissipative systems in the s-space, called fractional-order unstable dissipative systems (FOUDS). To this end, a signed distance function is defined between a complex number and the boundary of the fractional stability zone, which is composed of two rays, and a closed-form expression for this distance is obtained. With this function, both types of unstable dissipative systems are extended to the fractional-order case, and the resulting definition reduces to the classical one when $\alpha = 1$. For a given matrix, the definition gives explicit intervals of the fractional order in which the system is a FOUDS, and piecewise-linear FOUDS are designed with it to generate single-scroll and multi-scroll attractors.

This work is organized as follows. In Section 2, the problem statement is presented. In Section 3, elements of fractional calculus and stability of systems are provided, along with some results related to the complex straight line. In Section 4, the main results are given, and in Section 4.3 illustrative examples are presented. Finally, in Section 5, conclusions are drawn.

2 Problem statement

Consider the piecewise-linear fractional-order system of the form

$$D^{\alpha}x = Ax + B, \tag{1}$$

where $0 < \alpha < 2$, $x \in \mathbb{R}^3$ is the pseudo-state vector, $A \in \mathbb{R}^{3\times 3}$, and $B \in \mathbb{R}^3$ is a piecewise-defined vector as follows

$$B = \begin{cases} B_1 & \text{for } x \in \mathcal{D}_1, \\ B_2 & \text{for } x \in \mathcal{D}_2, \\ \vdots & \vdots \\ B_m & \text{for } x \in \mathcal{D}_m \end{cases} \tag{2}$$

where B will be designed to locate the equilibrium points $x_j^* = -A^{-1}B_j$ in a suitable way to generate multi-scroll attractors, with $\bigcup_{j=1}^{m} \mathcal{D}_j = \mathbb{R}^3$ and $\mathcal{D}_i \cap \mathcal{D}_j = \emptyset$ for $i \neq j$, $i, j = 1, \ldots, m$.

The idea is to consider the change of variable $s = \lambda^{\alpha}$, denoted by the mapping $s_{\alpha}(\lambda) = \lambda^{\alpha}$, with $\lambda \in \mathbb{C}$ and $0 < \alpha < 2$, and describe some topological properties of the transformed stability regions, with the aim of preserving the UDS structure for A. That is, the problem is to find the conditions that the zeros of the characteristic polynomial $\det(sI - A)$, now in the variable s, must satisfy so that the spectrum induces the manifold structure associated with the generation of multi-scroll attractors.

To achieve this, a new definition of unstable dissipative systems must be established for the spectrum of A, using the transformed stable and unstable subsets induced by s_{α}, and applied to the system (1).

3 Preliminaries

3.1 Fractional-order systems

Following Kilbas *et al.* [17], for any complex number z, $\mathrm{Re}(z) > 0$, the Euler's gamma function is defined as

$$\Gamma(z) := \int_0^\infty e^{-u} u^{z-1} du. \tag{3}$$

Notice that $\Gamma(z+1) = z\Gamma(z)$ and if $z = n$ is a positive integer then $\Gamma(n) = (n-1)!$. Now, if $n \in \mathbb{N}$ and $n-1 < \alpha < n$, where α is the commensurate order, the *Riemann–Liouville fractional-order derivative* is defined as

$${}_a^{RL}D_t^\alpha x(t) := \frac{1}{\Gamma(n-\alpha)} \frac{d^n}{dt^n} \int_a^t \frac{x(\tau)}{(t-\tau)^{\alpha-n+1}} d\tau, \tag{4}$$

where a and t are the limits of integration.

In the same way, the *Caputo fractional-order derivative* is defined as

$${}_a^{C}D_t^\alpha\, x(t) := \frac{1}{\Gamma(n-\alpha)} \int_a^t \frac{x^{(n)}(\tau)}{(t-\tau)^{\alpha+1-n}} d\tau,\ n-1 < \alpha < n, \tag{5}$$

where $n = \lceil \alpha \rceil$ and $x^{(n)}(\tau)$ denotes the classical n-th derivative of $x(\tau)$.

For the purpose of studying stability it is common to take $a = 0$ and to omit the labels C and RL. The two derivatives coincide when $x^{(k)}(0) = 0$ for $k = 0, \ldots, n-1$. In this work the Caputo derivative is used throughout.

A classical homogeneous fractional-order differential equation is given by [13, 20]

$$\sum_{j=0}^{n} a_j D^{(n-j)\alpha} y(t) = 0, \tag{6}$$

where $y(t)$ is a smooth Riemann integrable function, with $a_j \in \mathbb{R}$. Suppose that the system is of commensurate order α, that is, $\alpha_j = j\alpha$. Assuming without loss of generality that $a_0 = 1$, the change of variable $D^{j\alpha} y(t) = x_{j+1}(t)$, $j = 0, 1, \ldots, n-1$, allows the system (6) to be expressed as

$$\begin{bmatrix} D^\alpha x_1 \\ D^\alpha x_2 \\ \vdots \\ D^\alpha x_n \end{bmatrix} = \begin{bmatrix} 0 & 1 & 0 & \ldots & 0 \\ 0 & 0 & 1 & \ldots & 0 \\ \vdots & \vdots & \vdots & & \vdots \\ -a_n & -a_{n-1} & -a_{n-2} & \ldots & -a_1 \end{bmatrix} \begin{bmatrix} x_1 \\ x_2 \\ \vdots \\ x_n \end{bmatrix}, \tag{7}$$

whose dynamics is governed by the fractional-order characteristic pseudo-polynomial $q(\lambda^\alpha) = \sum_{j=0}^{n} a_j \lambda^{(n-j)\alpha}$.

In classic integer-order differential equations theory, the homogeneous system

$$\dot{x}(t) = Ax(t),$$

with $x \in \mathbb{R}^n$ and $A \in \mathbb{R}^{n \times n}$, is asymptotically stable if and only if $|\arg(\lambda)| > \frac{\pi}{2}$, for all eigenvalues λ of A. In the developed theory for fractional systems, there are

analogous results on stability, and the following theorems characterize them in terms of the spectrum of the system.

Theorem 1 (Matignon, 1996 [14]) *The FODE system*

$$D^\alpha x(t) = Ax(t), \;\; x(t_0) = x_0, \;\; 0 < \alpha < 2, \tag{8}$$

where $x \in \mathbb{R}^n$, is asymptotically stable if and only if $|\arg(\lambda_j)| > \frac{\pi}{2}$ for every root λ_j of $q(\lambda^\alpha) = \det(\lambda^\alpha I - A)$.

The change of variable $s = \lambda^\alpha$ induces the map $s_\alpha(\lambda) = \lambda^\alpha$. The principal sheet of its Riemann surface is defined for $-\pi < \arg(\lambda) < \pi$, and the corresponding s domain is $-\alpha\pi < \arg(s) < \alpha\pi$; the right half plane of this sheet corresponds to the region $-\alpha\frac{\pi}{2} < \arg(s) < \alpha\frac{\pi}{2}$ of the s-plane [20]. With this map, the stability of FODE systems and the stability zone can be described in the s-plane.

Theorem 2 (Matignon, 1996, 1998 [14, 15]) *The FODE system*

$$D^\alpha x(t) = Ax(t), \;\; x(t_0) = x_0, \;\; 0 < \alpha < 2, \tag{9}$$

where $x \in \mathbb{R}^n$, is asymptotically stable if and only if $|\arg(s_j)| > \alpha\frac{\pi}{2}$ for every root s_j of $q(s) = \det(sI - A)$, where $s = \lambda^\alpha$.

Theorem 2 is easier to apply than Theorem 1, since the test only requires the roots of the polynomial $\det(sI - A)$ and the comparison of their arguments with $\alpha\frac{\pi}{2}$.

In qualitative analysis, the stability zone for the spectrum of the pseudo-polynomial $q(\lambda^\alpha)$ is defined as

$$\mathbb{C}^- = \left\{\lambda \in \mathbb{C} \,:\, |\arg(\lambda)| > \frac{\pi}{2}\right\}, \tag{10}$$

while the stability zone for $q(s)$ is described by

$$\mathbb{C}_\alpha^- = \left\{\lambda \in \mathbb{C} \,:\, |\arg(\lambda)| > \alpha\frac{\pi}{2}\right\}, \tag{11}$$

via the change of variable $s = \lambda^\alpha$ (see figure 1). Thus, in the sense of Theorems 1 and 2, $q(\lambda^\alpha) = \sum_{j=0}^{n} a_j \lambda^{(n-j)\alpha}$ is stable with respect to $\mathbb{C}^-$ if and only if its associated integer-order polynomial $q(s) = \sum_{j=0}^{n} a_j s^{n-j}$ is stable with respect to $\mathbb{C}_\alpha^-$.

3.2 The complex straight line and distance

To compute distances in the complex plane, recall that there is a homeomorphism between $\mathbb{C}$ and $\mathbb{R}^2$ given by

$$\begin{aligned} h \,:\, \mathbb{C} &\to \mathbb{R}^2 \\ z = x + iy &\mapsto \begin{pmatrix} x \\ y \end{pmatrix} = \zeta, \end{aligned} \tag{12}$$

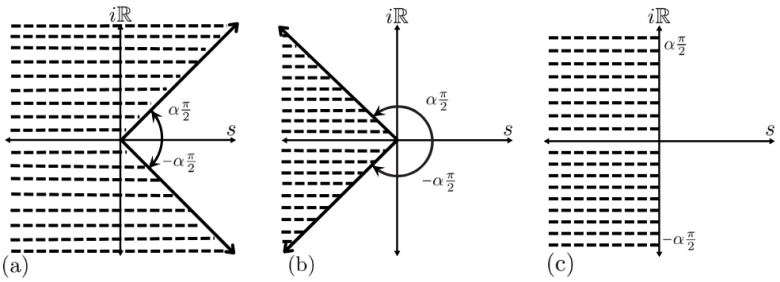


Fig. 1: Stability zones for $q(s)$ via the change $s = \lambda^\alpha$ for a) $0 < \alpha < 1$; b) $1 < \alpha < 2$; c) $\alpha = 1$.

which is an isometry between $\mathbb{C}$ with the modulus and $\mathbb{R}^2$ with the Euclidean norm [31, 32]. Thus, the analytic geometry of $\mathbb{R}^2$ can be used in the complex plane. Namely, the Euclidean distance between any pair of complex numbers z_1 and z_2, denoted by $d(z_1, z_2)$, is defined by

$$d(z_1, z_2) = |z_2 - z_1| \geq 0.$$

Additionally, for a complex z_0 and a nonempty subset $S \subset \mathbb{C}$, the distance between the point z_0 and the set S is given by

$$d(z_0, S) = \min_{a \in S} \{d(z_0, a)\}. \tag{13}$$

On the other hand, the straight line on the plane is given by

$$ax + by + c = 0, \tag{14}$$

and the distance between a point $\zeta_0 = (x_0, y_0)$ and the straight line (14) is given by

$$d(\zeta_0, \mathcal{L}) = \left| \frac{ax_0 + by_0 + c}{\sqrt{a^2 + b^2}} \right|,$$

where $\mathcal{L} = \left\{(x, y) \in \mathbb{R}^2 : ax + by + c = 0\right\}$. Under the identification $(a, b) \leftrightarrow w = a + ib$ of the line coefficients with a complex number, together with the map (12) for the points, the real straight line (14) admits the equivalent complex form given in the following result.

Lemma 3 *The straight line* (14) *in the real plane is equivalent to the complex straight line*

$$w\bar{z} + \bar{w}z + k = 0, \tag{15}$$

where $w = a + ib$ is fixed, z is the complex variable and $k = 2c$.

Consider a complex number $z_0 = \cos(\theta) + i\sin(\theta)$, with a fixed $0 < \theta < \pi$. By the map (12), the real straight line passing through the origin and containing the point $z_0 = (\cos\theta, \sin\theta)$ is given by

$$y - \sin\theta = \tan\theta(x - \cos\theta), \tag{16}$$

or equivalently,

$$x - \cot\theta\, y = 0,$$

and by Lemma 3, the equivalent complex straight line is given by

$$w\bar{z} + \bar{w}z = 0, \tag{17}$$

where $w = 1 - i\cot(\theta)$. Define now the set

$$\mathcal{L} = \{z \in \mathbb{C} \mid w\bar{z} + \overline{w}z + k = 0\}, \tag{18}$$

which consists of all points belonging to the straight line (15). The following result shows how to compute the distance between a complex point and a straight line.

Lemma 4 *The minimum distance between z_0 and all the points of $\mathcal{L}$ is given by*

$$d(z_0, \mathcal{L}) = \left| \frac{w\bar{z}_0 + \bar{w}z_0 + k}{2w} \right|, \tag{19}$$

where, for the line through the origin with slope $\tan\theta$, one has $w = 1 - i\cot\theta$.

Thus, the distance from any complex number z_0 to the straight line $\mathcal{L}$ equals the length of the orthogonal projection of z_0 onto the normal direction of $\mathcal{L}$.

4 Main results: fractional-order unstable dissipative systems

In this section, the subsets induced by s_α are described and a signed distance function is defined on them. This function is then used to define FOUDS, and two piecewise-linear examples are presented.

4.1 Topological description and signed distance function

Firstly, note that the complex set $\mathbb{C}$ can be written as the union of three disjoint subsets. Namely,

$$\mathbb{C} = \mathbb{C}^- \cup i\mathbb{R} \cup \mathbb{C}^+,$$

where $\mathbb{C}^-$ is the subset described in (10), $i\mathbb{R}$ is the imaginary axis, and

$$\mathbb{C}^+ = \left\{ z \in \mathbb{C} : |\arg(z)| < \frac{\pi}{2} \right\}.$$

Analogously, these three subsets are transformed by the map s_α and then the complex plane is also described as the union of three disjoint subsets as follows:

$$\mathbb{C} = \mathbb{C}_\alpha^- \cup i\mathbb{R}_\alpha \cup \mathbb{C}_\alpha^+,$$

where $\mathbb{C}_\alpha^-$ is the subset described in (11), $i\mathbb{R}_\alpha = \partial\mathbb{C}_\alpha^-$ is the imaginary folded axis $i\mathbb{R}$ via s_α, and

$$\mathbb{C}_\alpha^+ = \left\{ z \in \mathbb{C} \,:\, |\arg(z)| < \alpha\frac{\pi}{2} \right\}.$$

That is, the left open half plane $\mathbb{C}^-$ has been transformed homeomorphically (in the principal sheet of the Riemann surface, see [16, 17]) onto $\mathbb{C}_\alpha^-$ (see figure 2).

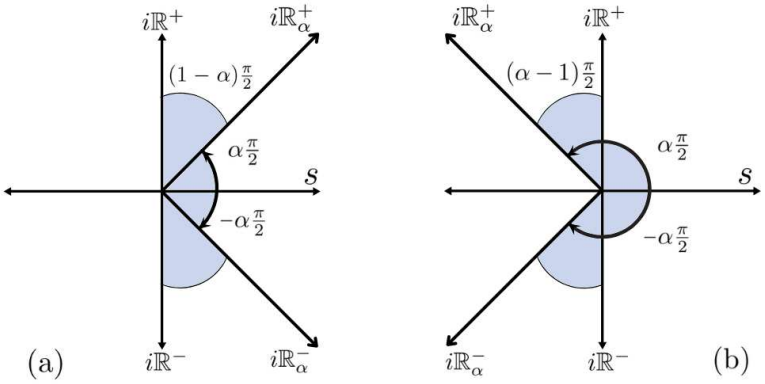


Fig. 2: Rotation of the imaginary rays by s_α with respect to their original position for a) $0 < \alpha < 1$; b) $1 < \alpha < 2$.

Next, the imaginary axis is written as the union of the imaginary rays and the origin in the form

$$i\mathbb{R} = i\mathbb{R}^+ \cup i\mathbb{R}^- \cup \{0\}.$$

Thus, the positive half-ray $i\mathbb{R}^+$ rotates under the action of the map s_α, acquiring an angle of $\alpha\frac{\pi}{2}$ measured from the positive real axis, to create the ray

$$i\mathbb{R}_\alpha^+ = \left\{ z \in \mathbb{C} \,:\, z = re^{i\alpha\frac{\pi}{2}},\, r > 0 \right\},$$

while the negative ray $i\mathbb{R}^-$ rotates under the action of the map by $-\alpha\frac{\pi}{2}$ measured from the positive real axis to create

$$i\mathbb{R}_\alpha^- = \left\{ z \in \mathbb{C} \,:\, z = re^{-i\alpha\frac{\pi}{2}},\, r > 0 \right\}.$$

Moreover,

$$\partial\mathbb{C}_\alpha^- = i\mathbb{R}_\alpha = i\mathbb{R}_\alpha^- \cup \{0\} \cup i\mathbb{R}_\alpha^+.$$

By the nature of the map s_α, the rays $i\mathbb{R}^+$ and $i\mathbb{R}^-$ are transformed into $i\mathbb{R}_\alpha^+$ and $i\mathbb{R}_\alpha^-$, respectively. That is, they have rotated by an angle of $(1-\alpha)\frac{\pi}{2}$ from their original position $\frac{\pi}{2}$ (the $i\mathbb{R}$ axis), for $0 < \alpha < 1$ (see (a) in figure 2). Analogously, if $1 < \alpha < 2$, the rays have rotated just an angle of $(\alpha-1)\frac{\pi}{2}$ from their original position (see (b) in figure 2).

Definition 1 For fixed $0 < \alpha < 2$ and $z \in \mathbb{C}$, the function δ is defined as

$$\delta(z) = \begin{cases} -d(z, i\mathbb{R}_\alpha) & \text{for } z \in \mathbb{C}_\alpha^-, \\ 0 & \text{for } z \in i\mathbb{R}_\alpha, \\ d(z, i\mathbb{R}_\alpha) & \text{for } z \in \mathbb{C}_\alpha^+, \end{cases} \tag{20}$$

where the function $d(\cdot, \cdot)$ is defined in (13).

The function δ is known as a *signed distance function*. In this sense, a complex number z will be considered to have a negative signed distance (or negative real part in the generalized sense) if $z \in \mathbb{C}_\alpha^-$, positive signed distance (or positive real part in the generalized sense) if $z \in \mathbb{C}_\alpha^+$, and zero distance if $z \in i\mathbb{R}_\alpha$.

Note that the distance d is not so easy to compute, since $i\mathbb{R}_\alpha$ is not a single-piece straight line but is composed of two conjugate rays, and some points have no orthogonal projection onto them (see figure 3). The following result gives this distance.

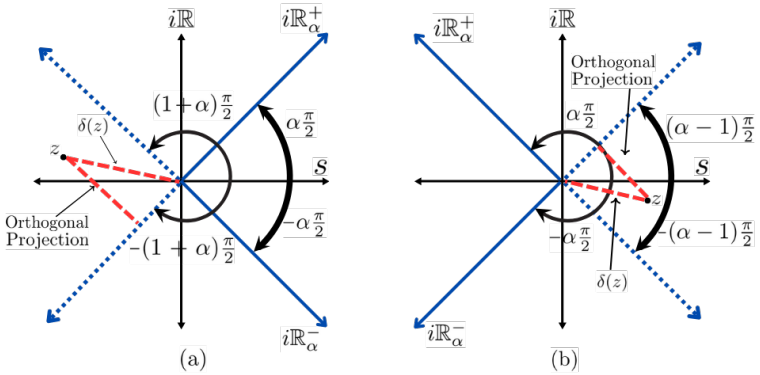


Fig. 3: Value of $\delta(z)$ for: a) $0 < \alpha < 1$ and $|\arg(z)| > (1+\alpha)\frac{\pi}{2}$; b) $1 < \alpha < 2$ and $|\arg(z)| < (\alpha-1)\frac{\pi}{2}$.

Theorem 5 *Let $z \in \mathbb{C}$ with $\mathrm{Im}(z) \geq 0$. The distance $d(z, i\mathbb{R}_\alpha)$, for $0 < \alpha < 1$, is given by*

$$d(z, i\mathbb{R}_\alpha) = \begin{cases} \left|\frac{w\bar{z}+\bar{w}z}{2w}\right| & \text{for } |\arg(z)| < (1+\alpha)\frac{\pi}{2} \\ |z| & \text{for } |\arg(z)| \geq (1+\alpha)\frac{\pi}{2} \end{cases}, \tag{21}$$

while for $1 < \alpha < 2$, the calculation is given by

$$d(z, i\mathbb{R}_\alpha) = \begin{cases} \left|\frac{w\bar{z}+\bar{w}z}{2w}\right| & \text{for } |\arg(z)| > (\alpha-1)\frac{\pi}{2} \\ |z| & \text{for } |\arg(z)| \leq (\alpha-1)\frac{\pi}{2} \end{cases}, \tag{22}$$

where $w = 1 - i\cot(\alpha\frac{\pi}{2})$. For $\mathrm{Im}(z) < 0$, $d(z, i\mathbb{R}_\alpha) = d(\bar{z}, i\mathbb{R}_\alpha)$.

Proof Since $i\mathbb{R}_\alpha$ is symmetric with respect to the real axis, $d(\bar{z}, i\mathbb{R}_\alpha) = d(z, i\mathbb{R}_\alpha)$, so it is enough to take $\mathrm{Im}(z) \geq 0$. In that case, the nearest point of $i\mathbb{R}_\alpha$ to z belongs to $\{0\} \cup i\mathbb{R}_\alpha^+$,

since for every point u of this ray, $|z-\bar{u}|^2 - |z-u|^2 = 4\,\mathrm{Im}(z)\,\mathrm{Im}(u) \geq 0$. The points of this ray are tu, with $t \geq 0$ and $u = e^{i\alpha\frac{\pi}{2}}$. The orthogonal projection of z onto the line that contains the ray is t^*u, with $t^* = \mathrm{Re}(z\bar{u})$, and it belongs to the ray if and only if $t^* \geq 0$, that is, if $|\arg(z) - \alpha\frac{\pi}{2}| \leq \frac{\pi}{2}$. In that case the distance is the length of the orthogonal projection, given by Lemma 4 with $\theta = \alpha\frac{\pi}{2}$. Otherwise $t^* < 0$, the distance from z to tu increases with $t \geq 0$, and the minimum is $|z|$, attained at the origin. For $0 < \alpha < 1$ and $0 \leq \arg(z) \leq \pi$, the condition $|\arg(z) - \alpha\frac{\pi}{2}| \leq \frac{\pi}{2}$ is equivalent to $\arg(z) \leq (1+\alpha)\frac{\pi}{2}$, which gives (21). For $1 < \alpha < 2$ it is equivalent to $\arg(z) \geq (\alpha-1)\frac{\pi}{2}$, which gives (22). □

Remark 1 In terms of the analytic geometry, for $0 < \alpha < 2$ and $\theta = \alpha\frac{\pi}{2}$, the ray $i\mathbb{R}_\alpha^+$ of the straight line passing through the origin and the point $z_1 = \cos(\alpha\frac{\pi}{2}) + i\sin(\alpha\frac{\pi}{2})$, is expressed as

$$i\mathbb{R}_\alpha^+ = \left\{ z \in \mathbb{C} \,|\, w\bar{z} + \bar{w}z = 0,\ \mathrm{Im}(z) > 0, w = 1 - i\cot(\alpha\frac{\pi}{2}) \right\}.$$

Remark 2 Note that if $\alpha = 1$, the signed distance function δ reduces to the real part, $\delta(z) = \mathrm{Re}(z)$.

4.2 Generalization to fractional-order UDS

With the signed distance function and Theorem 5, the unstable dissipative systems of [5, 6] are generalized to FODE systems in the s-space.

Definition 2 Consider the FODE system

$$D^\alpha x = Ax, \tag{23}$$

where $A = (a_{ij}) \in \mathbb{R}^{3\times 3}$ and $\alpha \in (0,2)$. For $j = 1,2,3$, let s_j be the zeros of the characteristic polynomial $q(s) = \det(sI - A)$ of A. Suppose that

$$\sum_{j=1}^{3} \delta(s_j) < 0. \tag{24}$$

Then the system (23) is said to be:

1. A fractional-order unstable dissipative system of type I (*FOUDS-I*) if and only if $s_1 \in \mathbb{R}^+$ and $s_2, s_3 \in \mathbb{C}_\alpha^-$, with $s_2 = \bar{s}_3$.
2. A fractional-order unstable dissipative system of type II (*FOUDS-II*) if and only if $s_1 \in \mathbb{R}^-$ and $s_2, s_3 \in \mathbb{C}_\alpha^+$, with $s_2 = \bar{s}_3$.

The inequality (24) is called *dissipativity condition*. The conditions i) and ii) are equivalent to requiring a non-degenerate saddle-focus equilibrium point, where $\delta(s_1)\delta(s_2) < 0$. In addition, if $s_2 = \bar{s}_3 = \sigma + i\eta$, it is required that $|\eta| \gg |\sigma|$, and the eigenspaces associated with each equilibrium inside $\mathcal{D}_j$ must intersect transversally with $\partial\mathcal{D}_{j-1}$ and $\partial\mathcal{D}_{j+1}$.

Remark 3 The condition (24) is the counterpart, in the s-plane, of the dissipativity condition of the unstable dissipative systems [5, 6], and for $\alpha = 1$ it reduces to $\mathrm{Tr}(A) < 0$ (Remark 2). For $\alpha \neq 1$, the condition is a property of the spectrum of A only.

Remark 4 The roots s_j of $\det(sI - A)$ do not depend on α, only the boundary $i\mathbb{R}_\alpha$ that separates $\mathbb{C}_\alpha^-$ from $\mathbb{C}_\alpha^+$ does. Since a positive real root always lies in $\mathbb{C}_\alpha^+$ and a negative one in $\mathbb{C}_\alpha^-$, the matrix A of a UDS of type I defines a FOUDS-I, and the matrix of a UDS of type II defines a FOUDS-II, for the values of α at which the conditions of Definition 2 hold. In both cases, the dimensions of the stable and unstable manifolds are the same as in the integer-order system.

4.3 Generating multi-scroll attractors in PWL-FOUDS

In this section, two examples of piecewise-linear FOUDS are presented, one of each type. For each example, the valid interval of the fractional order α is determined from the conditions of Definition 2, and the dynamics of the resulting attractor are examined through bifurcation diagrams. The numerical results were obtained with the Adams–Bashforth–Moulton predictor-corrector method with full memory [33].

4.3.1 FOUDS-I

Consider the fractional-order system

$$D^\alpha x = \begin{bmatrix} 0 & 1 & 0 \\ 0 & 0 & 1 \\ 2 & -10 & -1 \end{bmatrix} x + B, \tag{25}$$

with

$$B = \begin{cases} B_1 = [0,0,0]^T & \text{for } x \in \mathcal{D}_1, \\ B_2 = [0,0,-10]^T & \text{for } x \in \mathcal{D}_2, \end{cases} \tag{26}$$

where both regions $\mathcal{D}_1$ and $\mathcal{D}_2$ are defined by the boundary $x_1 = 1$, that is,

$$\mathcal{D}_1 = \left\{ x \in \mathbb{R}^3 : x_1 < 1 \right\},$$
$$\mathcal{D}_2 = \left\{ x \in \mathbb{R}^3 : x_1 \geq 1 \right\}.$$

The vectors B_j are chosen so that the equilibrium points $x_j^* = -A^{-1}B_j$ are located along the x_1 axis, at

$$x_1^* = (0,0,0)^T,$$
$$x_2^* = (5,0,0)^T.$$

The characteristic polynomial of the system $q(s) = s^3 + s^2 + 10s - 2$ has roots $s_1 = 0.1954$ and $s_{2,3} = -0.5977 \pm 3.1427i$, which satisfy condition (i) of Definition 2. Definition 2 requires both the membership condition $s_{2,3} \in \mathbb{C}_\alpha^-$ and the dissipativity condition (24); the valid interval of α is the intersection of the intervals obtained from each one.

The membership condition requires $|\arg(s_{2,3})| > \alpha\frac{\pi}{2}$. Since

$$\begin{aligned}|\arg(s_{2,3})| &= \arctan\left(\frac{\mathrm{Im}(s_{2,3})}{\mathrm{Re}(s_{2,3})}\right) + \pi,\\ &= \arctan\left(-\frac{3.1427}{0.5977}\right) + \pi,\\ &= 1.7587 \text{ rad},\end{aligned}$$

the condition $1.7587 > \alpha\frac{\pi}{2}$ gives $\alpha < 1.7587\frac{2}{\pi}$, so the membership condition holds on

$$0 < \alpha < 1.1196.$$

To verify the dissipativity condition (24), recall that $w = 1 - i\cot(\alpha\frac{\pi}{2})$, with modulus $|w| = 1/\sin(\alpha\frac{\pi}{2})$. Since the projection formula from Theorem 5 requires the computation of $\mathrm{Re}(w\bar{s}_j)$, these quantities are computed first. For $s_1 = 0.1954$, one has $\bar{s}_1 = 0.1954$, so

$$\begin{aligned}w\bar{s}_1 &= \left(1 - i\cot\left(\alpha\frac{\pi}{2}\right)\right)(0.1954),\\ &= 0.1954 - 0.1954\cot\left(\alpha\frac{\pi}{2}\right)i,\end{aligned}$$

giving $\mathrm{Re}(w\bar{s}_1) = 0.1954$. For $s_2 = -0.5977 + 3.1427i$, one has $\bar{s}_2 = -0.5977 - 3.1427i$, which gives

$$\begin{aligned}w\bar{s}_2 &= \left(1 - i\cot\left(\alpha\frac{\pi}{2}\right)\right)(-0.5977 - 3.1427i),\\ &= \left(-0.5977 - 3.1427\cot\left(\alpha\frac{\pi}{2}\right)\right) + \left(-3.1427 + 0.5977\cot\left(\alpha\frac{\pi}{2}\right)\right)i,\end{aligned}$$

giving $\mathrm{Re}(w\bar{s}_2) = -0.5977 - 3.1427\cot\left(\alpha\frac{\pi}{2}\right)$. By conjugate symmetry $\mathrm{Re}(w\bar{s}_3) = \mathrm{Re}(w\bar{s}_2) = -0.5977 - 3.1427\cot\left(\alpha\frac{\pi}{2}\right)$. The verification of condition (24) is divided into multiple cases determined by which branch of Theorem 5 applies to each eigenvalue, according to the value of α.

For $0 < \alpha \leq 0.1196$, since $\alpha \leq 0.1196$ implies $(1+\alpha)\frac{\pi}{2} \leq (1+0.1196)\frac{\pi}{2} = 1.7587$, it follows that $|\arg(s_{2,3})| = 1.7587 \geq (1+\alpha)\frac{\pi}{2}$ and, by the second branch of (21), $d(s_{2,3}, i\mathbb{R}_\alpha) = |s_{2,3}|$, where

$$\begin{aligned}|s_{2,3}| &= \sqrt{(-0.5977)^2 + (3.1427)^2},\\ &= \sqrt{0.3572 + 9.8766},\\ &= \sqrt{10.2338},\\ &= 3.1990.\end{aligned}$$

For s_1, since $|\arg(s_1)| = 0 < (1+\alpha)\frac{\pi}{2}$ for all $\alpha > 0$, the projection branch of (21) gives

$$\begin{aligned} d(s_1, i\mathbb{R}_\alpha) &= \frac{|\operatorname{Re}(w\bar{s}_1)|}{|w|}, \\ &= 0.1954 \sin\left(\alpha\frac{\pi}{2}\right). \end{aligned}$$

Since $s_1 \in \mathbb{C}_\alpha^+$ and $s_{2,3} \in \mathbb{C}_\alpha^-$, applying Definition 1 gives $\delta(s_1) = 0.1954 \sin\left(\alpha\frac{\pi}{2}\right)$ and $\delta(s_{2,3}) = -3.1990$, so

$$\sum_{j=1}^{3} \delta(s_j) = 0.1954 \sin\left(\alpha\frac{\pi}{2}\right) - 6.3980,$$

and since $\sin\left(\alpha\frac{\pi}{2}\right)$ is increasing and $\alpha \leq 0.1196$ in this interval, it follows that $\sin\left(\alpha\frac{\pi}{2}\right) \leq \sin\left(0.1196\frac{\pi}{2}\right) = 0.1868$, which gives

$$\begin{aligned} \sum_{j=1}^{3} \delta(s_j) &\leq 0.1954(0.1868) - 6.3980, \\ &\leq 0.0365 - 6.3980, \\ &\leq -6.3615. \end{aligned}$$

For $0.1196 < \alpha < 1$, since $\alpha > 0.1196$ implies $(1+\alpha)\frac{\pi}{2} > (1+0.1196)\frac{\pi}{2} = 1.7587$, it follows that $|\arg(s_{2,3})| = 1.7587 < (1+\alpha)\frac{\pi}{2}$, so the projection formula (21) applies to all eigenvalues. Given that $\cot\left(\alpha\frac{\pi}{2}\right) > 0$ for $0 < \alpha < 1$, it follows that $-0.5977 - 3.1427\cot\left(\alpha\frac{\pi}{2}\right) < 0$, so $|\operatorname{Re}(w\bar{s}_{2,3})| = 0.5977 + 3.1427\cot\left(\alpha\frac{\pi}{2}\right)$. Applying the projection formula yields

$$\begin{aligned} d\left(s_1, i\mathbb{R}_\alpha\right) &= \frac{0.1954}{1/\sin\left(\alpha\frac{\pi}{2}\right)}, \\ &= 0.1954 \sin\left(\alpha\frac{\pi}{2}\right), \end{aligned}$$

and

$$\begin{aligned} d\left(s_{2,3}, i\mathbb{R}_\alpha\right) &= \frac{0.5977 + 3.1427\cot\left(\alpha\frac{\pi}{2}\right)}{1/\sin\left(\alpha\frac{\pi}{2}\right)}, \\ &= \left(0.5977 + 3.1427\cot\left(\alpha\frac{\pi}{2}\right)\right)\sin\left(\alpha\frac{\pi}{2}\right). \end{aligned}$$

Applying Definition 1, $\delta(s_1) = 0.1954 \sin\left(\alpha\frac{\pi}{2}\right)$ and $\delta(s_{2,3}) = -\left(0.5977 + 3.1427\cot\left(\alpha\frac{\pi}{2}\right)\right)\sin\left(\alpha\frac{\pi}{2}\right)$, then

$$\sum_{j=1}^{3}\delta(s_j) = \sin\left(\alpha\frac{\pi}{2}\right)\left(-1 - 6.2854\cot\left(\alpha\frac{\pi}{2}\right)\right).$$

Given that $\sin\left(\alpha\frac{\pi}{2}\right) > 0$ and $\cot\left(\alpha\frac{\pi}{2}\right) > 0$ for $0.1196 < \alpha < 1$, the expression $\left(-1 - 6.2854\cot\left(\alpha\frac{\pi}{2}\right)\right)$ is strictly negative, and therefore $\sum_{j=1}^{3}\delta(s_j) < 0$. Note that as $\alpha \to 1$, $\cot\left(\alpha\frac{\pi}{2}\right) \to 0$, and the expression reduces to $\sin\left(\frac{\pi}{2}\right)(-1) = \mathrm{Tr}(A) = -1$, consistent with Remark 2.

For $1 < \alpha < 1.1196$, the distance calculation is given by (22). Since $|\arg(s_1)| = 0 \le (\alpha - 1)\frac{\pi}{2}$ for $1 < \alpha < 2$, it follows that $d(s_1, i\mathbb{R}_\alpha) = |s_1| = 0.1954$. Given that $|\arg(s_{2,3})| = 1.7587 > (\alpha - 1)\frac{\pi}{2}$ throughout this interval, the projection expression of (22) applies to $s_{2,3}$. Here $\cot\left(\alpha\frac{\pi}{2}\right) \in (-0.1902, 0)$, so $\mathrm{Re}(w\bar{s}_{2,3}) = -0.5977 - 3.1427\cot\left(\alpha\frac{\pi}{2}\right) < 0$, giving $|\mathrm{Re}\,(w\bar{s}_{2,3})| = \left|-0.5977 - 3.1427\cot\left(\alpha\frac{\pi}{2}\right)\right|$.

Applying the projection formula gives

$$d\left(s_{2,3}, i\mathbb{R}_\alpha\right) = \left|-0.5977 - 3.1427\cot\left(\alpha\frac{\pi}{2}\right)\right|\sin\left(\alpha\frac{\pi}{2}\right).$$

Applying Definition 1, $\delta(s_1) = 0.1954$ and $\delta(s_{2,3}) = -\left|-0.5977 - 3.1427\cot\left(\alpha\frac{\pi}{2}\right)\right|\sin\left(\alpha\frac{\pi}{2}\right)$, so

$$\sum_{j=1}^{3}\delta(s_j) = 0.1954 - 2\left|-0.5977 - 3.1427\cot\left(\alpha\frac{\pi}{2}\right)\right|\sin\left(\alpha\frac{\pi}{2}\right),$$

and since $\cot\left(\alpha\frac{\pi}{2}\right) \in (-0.1902, 0)$, it follows that $-3.1427\cot\left(\alpha\frac{\pi}{2}\right) \in (0, 0.5977)$, so $-0.5977 - 3.1427\cot\left(\alpha\frac{\pi}{2}\right) \in (-0.5977, 0)$, giving $\left|-0.5977 - 3.1427\cot\left(\alpha\frac{\pi}{2}\right)\right| \in (0, 0.5977)$.

At $\alpha \to 1^+$, the sum approaches $0.1954 - 2(0.5977)(1) = -1 = \mathrm{Tr}(A) < 0$, consistent with Remark 2. However, as α increases toward 1.1196, the focus $s_{2,3}$ approaches the boundary $i\mathbb{R}_\alpha$, so its stabilizing contribution $\delta(s_{2,3}) \to 0^-$, while the destabilizing contribution $\delta(s_1) = 0.1954 > 0$ remains fixed. Consequently the sum is increasing on this subinterval and crosses zero when

$$0.1954 = 2\left|-0.5977 - 3.1427\cot\left(\alpha\frac{\pi}{2}\right)\right|\sin\left(\alpha\frac{\pi}{2}\right),$$

which occurs at $\alpha \approx 1.1002$. Therefore the dissipativity condition (24) holds only for $0 < \alpha < 1.1002$, a strictly smaller interval than the membership condition.

Intersecting the two intervals, both requirements of Definition 2 are satisfied if and only if

$$0 < \alpha < 1.1002.$$

In this example, the upper limit of the interval is given by the dissipativity condition, which fails at $\alpha \approx 1.1002$, while $s_{2,3}$ remains in $\mathbb{C}_\alpha^-$ up to $\alpha = 1.1196$. The reason is

that the contribution of $s_{2,3}$ to the sum (24) tends to zero as $s_{2,3}$ approaches $i\mathbb{R}_\alpha$. For this example, $\alpha = 1.05$ is used.

Figure 4 shows the attractor of the FOUDS-I system (25)–(26) for $\alpha = 1.05$, with initial conditions $x_0 = (0.9, 0, 0)^T$ and $\dot{x}_0 = (0, 0, 0)^T$. At each equilibrium, the positive real eigenvalue $s_1 = 0.1954 \in \mathbb{C}_\alpha^+$ is associated with a one-dimensional unstable manifold W^u, and the complex conjugate pair $s_{2,3} = -0.5977 \pm 3.1427i \in \mathbb{C}_\alpha^-$ with a two-dimensional stable manifold W^s, along which the trajectory rotates. The switching law (26) moves the trajectory between $\mathcal{D}_1$ and $\mathcal{D}_2$, and the dissipativity condition holds with $\sum_{j=1}^{3} \delta(s_j) = -0.5032$. The projections in Figure 5 show a single-scroll attractor.attractor.

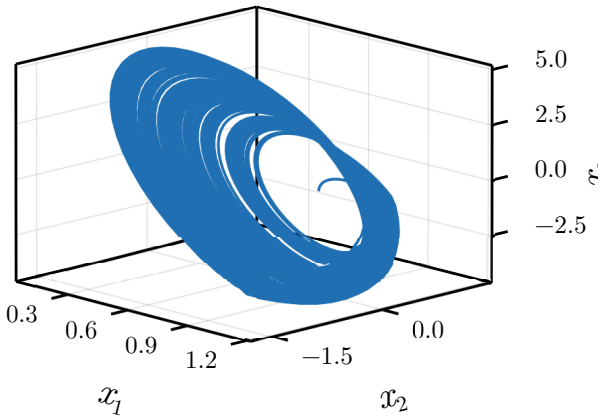
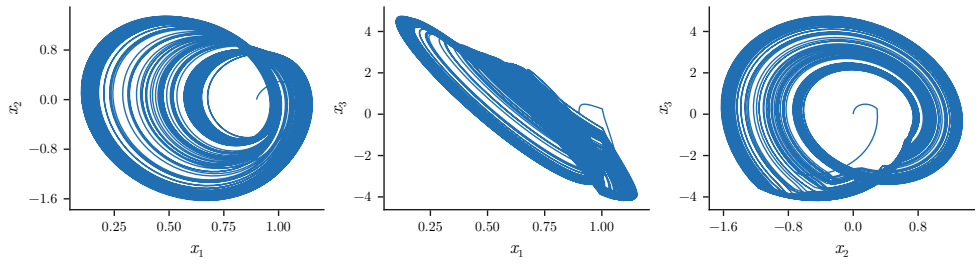


Fig. 4: Attractor of the FOUDS-I system (25)–(26) for $\alpha = 1.05$.



(a) (b) (c)

Fig. 5: Projections of the FOUDS-I system (25)–(26) for $\alpha = 1.05$: a) (x_1, x_2) plane; b) (x_1, x_3) plane; c) (x_2, x_3) plane.

The dynamical behavior of the FOUDS-I system (25)–(26) as the fractional order varies is summarized in Figure 6, which shows the local maxima of the state x_1 as

a function of α. For each value of α, the system was integrated with the Adams–Bashforth–Moulton predictor-corrector method, the initial transient was discarded, and the successive maxima of x_1 were recorded on the resulting attractor. The diagram is shown for $\alpha \geq 0.80$. Up to $\alpha \approx 0.93$ it shows a single branch slightly above $x_1 = 1$; beyond this value the maxima spread over a continuous range, which indicates irregular dynamics. The value $\alpha = 1.05$ used in Figures 4–5 lies in this range. The diagram ends at the limit $\alpha = 1.1002$ of the valid interval.

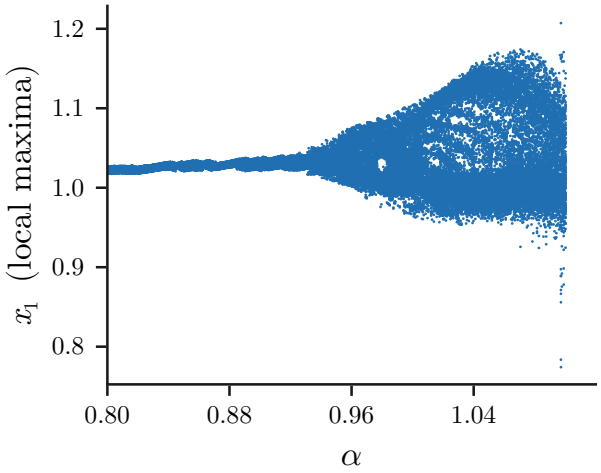


Fig. 6: Bifurcation diagram of the FOUDS-I system (25)–(26): local maxima of x_1 versus the fractional order α.

4.3.2 FOUDS-II

Consider the fractional-order system given by

$$D^{\alpha}x = \begin{bmatrix} 0 & 1 & 0 \\ 0 & 0 & 1 \\ -1.5 & -1 & -1 \end{bmatrix} x + B, \tag{27}$$

with

$$B = \begin{cases} B_1 = [0, 0, -2.25]^T & \text{for } x \in \mathcal{D}_1, \\ B_2 = [0, 0, -0.75]^T & \text{for } x \in \mathcal{D}_2, \\ B_3 = [0, 0, 0.75]^T & \text{for } x \in \mathcal{D}_3, \\ B_4 = [0, 0, 2.25]^T & \text{for } x \in \mathcal{D}_4, \end{cases} \tag{28}$$

where the regions $\mathcal{D}_j$ are defined by the switching boundaries $x_1 \in \{-1, 0, 1\}$, that is,

$$\mathcal{D}_1 = \left\{ x \in \mathbb{R}^3 : x_1 < -1 \right\},$$

$$\mathcal{D}_2 = \left\{x \in \mathbb{R}^3 : -1 \leq x_1 < 0\right\},$$
$$\mathcal{D}_3 = \left\{x \in \mathbb{R}^3 : 0 \leq x_1 < 1\right\},$$
$$\mathcal{D}_4 = \left\{x \in \mathbb{R}^3 : 1 \leq x_1\right\}.$$

The vectors B_j are chosen so that the equilibrium points $x_j^* = -A^{-1}B_j$ are located along the x_1 axis at

$$x_1^* = (-1.5, 0, 0)^T,$$
$$x_2^* = (-0.5, 0, 0)^T,$$
$$x_3^* = (0.5, 0, 0)^T,$$
$$x_4^* = (1.5, 0, 0)^T.$$

The characteristic polynomial of the system $q(s) = s^3 + s^2 + s + 1.5$ has roots $s_1 = -1.2041$ and $s_{2,3} = 0.1020 \pm 1.1115i$, which satisfy condition (ii) of Definition 2. As in the previous example, the valid interval is the intersection of the intervals given by the membership condition $s_{2,3} \in \mathbb{C}_\alpha^+$ and the dissipativity condition (24).

Since $s_{2,3}$ has positive real part, membership in $\mathbb{C}_\alpha^+$ requires that $|\arg(s_{2,3})| < \alpha\frac{\pi}{2}$. Thus

$$\begin{aligned}|\arg(s_{2,3})| &= \arctan\left(\frac{\mathrm{Im}(s_{2,3})}{\mathrm{Re}(s_{2,3})}\right),\\ &= \arctan\left(\frac{1.1115}{0.1020}\right),\\ &= 1.4793 \text{ rad},\end{aligned}$$

and the condition $1.4793 < \alpha\frac{\pi}{2}$ gives $\alpha > 1.4793\frac{2}{\pi}$, so the membership condition holds on

$$\alpha > 0.9417.$$

Furthermore, since $s_1 = -1.2041 < 0$, one has $|\arg(s_1)| = \pi > \alpha\frac{\pi}{2}$ for all $\alpha < 2$, so $s_1 \in \mathbb{C}_\alpha^-$ throughout.

To verify the dissipativity condition (24), recall that $w = 1 - i\cot\left(\alpha\frac{\pi}{2}\right)$, with modulus $|w| = 1/\sin\left(\alpha\frac{\pi}{2}\right)$. Since the projection formula from Theorem 5 requires the computation of $\mathrm{Re}\,(w\bar{s}_j)$, these quantities are computed first. For $s_1 = -1.2041$, one has $\bar{s}_1 = -1.2041$, so

$$\begin{aligned}w\bar{s}_1 &= \left(1 - i\cot\left(\alpha\frac{\pi}{2}\right)\right)(-1.2041),\\ &= -1.2041 + 1.2041\cot\left(\alpha\frac{\pi}{2}\right)i,\end{aligned}$$

giving $\mathrm{Re}\,(w\bar{s}_1) = -1.2041$. For $s_2 = 0.1020 + 1.1115i$, one has $\bar{s}_2 = 0.1020 - 1.1115i$, which gives

$$\begin{aligned} w\bar{s}_2 &= \left(1 - i\cot\left(\alpha\frac{\pi}{2}\right)\right)(0.1020 - 1.1115i)\,, \\ &= \left(0.1020 - 1.1115\cot\left(\alpha\frac{\pi}{2}\right)\right) + \left(-1.1115 - 0.1020\cot\left(\alpha\frac{\pi}{2}\right)\right)i, \end{aligned}$$

giving $\mathrm{Re}\,(w\bar{s}_2) = 0.1020 - 1.1115\cot\left(\alpha\frac{\pi}{2}\right)$. By conjugate symmetry $\mathrm{Re}\,(w\bar{s}_3) = \mathrm{Re}\,(w\bar{s}_2)$. Since the valid window crosses $\alpha = 1$, the verification of condition (24) is divided into two cases determined by which branch of Theorem 5 applies to each eigenvalue.

For $0.9417 < \alpha < 1$, the distance is given by (21). Since $|\arg(s_1)| = \pi \geq (1+\alpha)\frac{\pi}{2}$ for $\alpha < 1$, the second branch of (21) gives

$$\begin{aligned} d\,(s_1, i\mathbb{R}_\alpha) &= |s_1|\,, \\ &= \sqrt{(-1.2041)^2}, \\ &= 1.2041. \end{aligned}$$

Given that $|\arg(s_{2,3})| = 1.4793 < (1+\alpha)\frac{\pi}{2}$ throughout this interval, the projection branch of (21) applies to $s_{2,3}$. Here $\cot\left(\alpha\frac{\pi}{2}\right) \in (0, 0.0918)$, so

$$\begin{aligned} d\,(s_{2,3}, i\mathbb{R}_\alpha) &= \frac{|\mathrm{Re}(w\bar{s}_{2,3})|}{|w|}, \\ &= \left|0.1020 - 1.1115\cot\left(\alpha\frac{\pi}{2}\right)\right|\sin\left(\alpha\frac{\pi}{2}\right). \end{aligned}$$

Since $s_1 \in \mathbb{C}_\alpha^-$ and $s_{2,3} \in \mathbb{C}_\alpha^+$, applying Definition 1 gives $\delta(s_1) = -1.2041$ and $\delta(s_{2,3}) = \left|0.1020 - 1.1115\cot\left(\alpha\frac{\pi}{2}\right)\right|\sin\left(\alpha\frac{\pi}{2}\right)$, so

$$\sum_{j=1}^{3}\delta(s_j) = -1.2041 + 2\left|0.1020 - 1.1115\cot\left(\alpha\frac{\pi}{2}\right)\right|\sin\left(\alpha\frac{\pi}{2}\right).$$

Since $\cot\left(\alpha\frac{\pi}{2}\right) \in (0, 0.0918)$ and $\sin\left(\alpha\frac{\pi}{2}\right) \leq 1$ on this interval, the positive contribution remains below 0.21, so

$$\sum_{j=1}^{3}\delta(s_j) < -0.99.$$

For $1 < \alpha < 1.2691$, the distance is given by (22). Since $|\arg(s_1)| = \pi > (\alpha - 1)\frac{\pi}{2}$ throughout this interval, the projection expression of (22) applies to s_1,

$$d\,(s_1, i\mathbb{R}_\alpha) = \frac{|\mathrm{Re}(w\bar{s}_1)|}{|w|},$$

$$= 1.2041 \sin\left(\alpha\frac{\pi}{2}\right).$$

Given that $|\arg(s_{2,3})| = 1.4793 > (\alpha - 1)\,\frac{\pi}{2}$ throughout this interval, the projection expression of (22) also applies to $s_{2,3}$. Here $\cot\left(\alpha\frac{\pi}{2}\right) \in (-0.4498, 0)$, so

$$d\left(s_{2,3}, i\mathbb{R}_\alpha\right) = \left|0.1020 - 1.1115\cot\left(\alpha\frac{\pi}{2}\right)\right| \sin\left(\alpha\frac{\pi}{2}\right).$$

Applying Definition 1, $\delta(s_1) = -1.2041\sin\left(\alpha\frac{\pi}{2}\right)$ and $\delta(s_{2,3}) = \left|0.1020 - 1.1115\cot\left(\alpha\frac{\pi}{2}\right)\right|\sin\left(\alpha\frac{\pi}{2}\right)$, so

$$\sum_{j=1}^{3}\delta(s_j) = \sin\left(\alpha\frac{\pi}{2}\right)\left[-1.2041 + 2\left|0.1020 - 1.1115\cot\left(\alpha\frac{\pi}{2}\right)\right|\right].$$

At $\alpha \to 1^+$, $\cot\left(\alpha\frac{\pi}{2}\right) \to 0$, and the sum approaches $\sin\left(\frac{\pi}{2}\right)[-1.2041 + 2\,(0.1020)] \approx -1 = \mathrm{Tr}(A) < 0$, consistent with Remark 2. As α increases, $\cot\left(\alpha\frac{\pi}{2}\right) < 0$ grows in magnitude, so $\left|0.1020 - 1.1115\cot\left(\alpha\frac{\pi}{2}\right)\right|$ increases, and the sum $-1.2041 + 2\left|0.1020 - 1.1115\cot\left(\alpha\frac{\pi}{2}\right)\right|$ rises toward zero, crossing it at $\alpha \approx 1.2691$. Therefore the dissipativity condition (24) holds only for $\alpha < 1.2691$.

Intersecting the membership interval $\alpha > 0.9417$ with the dissipativity interval $\alpha < 1.2691$, both requirements of Definition 2 are satisfied if and only if

$$0.9417 < \alpha < 1.2691.$$

Unlike the interval of the FOUDS-I example, this window has two limits. The lower limit is given by the membership condition, when $s_{2,3}$ enters $\mathbb{C}_\alpha^+$, and the upper limit by the dissipativity condition, when the sum (24) becomes positive.

Figure 7 shows the attractor of the FOUDS-II system (27)–(28) for $\alpha = 1.1$, with initial conditions $x_0 = (0.1, 0, 0)^T$ and $\dot{x}_0 = (0, 0, 0)^T$. At each equilibrium, the negative real eigenvalue $s_1 = -1.2041 \in \mathbb{C}_\alpha^-$ is associated with a one-dimensional stable manifold W^s, and the complex conjugate pair $s_{2,3} = 0.1020 \pm 1.1115i \in \mathbb{C}_\alpha^+$ with a two-dimensional unstable manifold W^u, along which the trajectory spirals outward. The switching law (28) moves the trajectory among the regions $\mathcal{D}_1, \ldots, \mathcal{D}_4$, whose equilibria $x_1^*, \ldots, x_4^*$ are the centers of the four scrolls, and the dissipativity condition holds with $\sum_{j=1}^{3}\delta(s_j) = -0.6399$. The projections in the Figure 8 shows a four-scroll attractor.

The dynamical behavior of the FOUDS-II system (27)–(28) as the fractional order varies is summarized in Figure 9, which shows the local maxima of the state x_1 as a function of α over the valid window $0.9417 < \alpha < 1.2691$ established above. For each value of α, the system was integrated with the Adams–Bashforth–Moulton predictor-corrector method, the initial transient was discarded, and the successive maxima of x_1 were recorded on the resulting attractor. The diagram displays four bands of maxima, one for each region $\mathcal{D}_1, \ldots, \mathcal{D}_4$, corresponding to the four scrolls of the attractor. The bands broaden and intermingle as α increases. It should be noted that a bounded

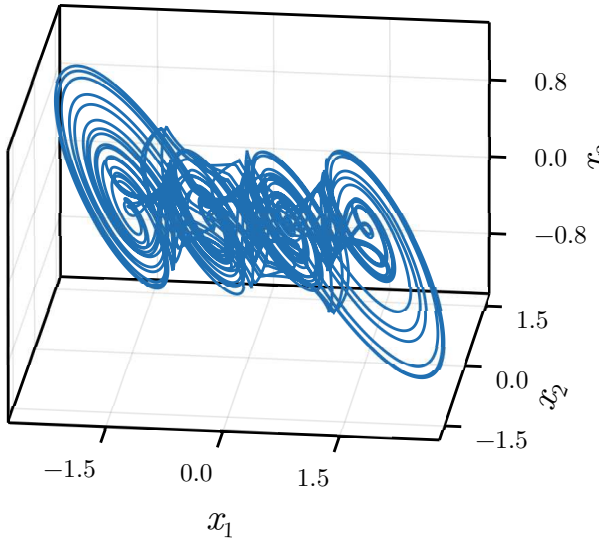
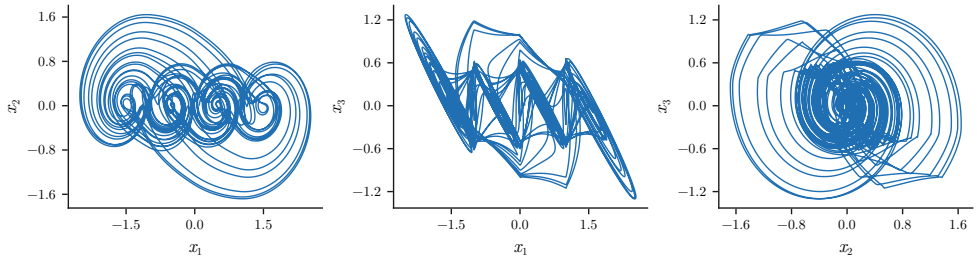


Fig. 7: Attractor of the FOUDS-II system (27)–(28) for $\alpha = 1.1$.



(a) (b) (c)

Fig. 8: Projections of the FOUDS-II system (27)–(28) for $\alpha = 1.1$: a) (x_1, x_2) plane; b) (x_1, x_3) plane; c) (x_2, x_3) plane.

four-scroll attractor is generated only up to $\alpha \approx 1.15$; beyond this value the trajectory becomes unbounded, and the diagram is empty up to the analytic limit $\alpha = 1.2691$. Hence, the conditions of Definition 2 are not sufficient for the existence of a bounded attractor.

5 Conclusions

Unstable dissipative systems were generalized to the fractional-order case by means of the map s_α, which transforms the stability zone $\mathbb{C}^-$ onto $\mathbb{C}_\alpha^-$, and a signed distance function to the boundary $i\mathbb{R}_\alpha$. With this function, Definition 2 gives a criterion for the design of piecewise-linear fractional-order systems that generate single-scroll and multi-scroll attractors, and it reduces to the classical definition when $\alpha = 1$. In the

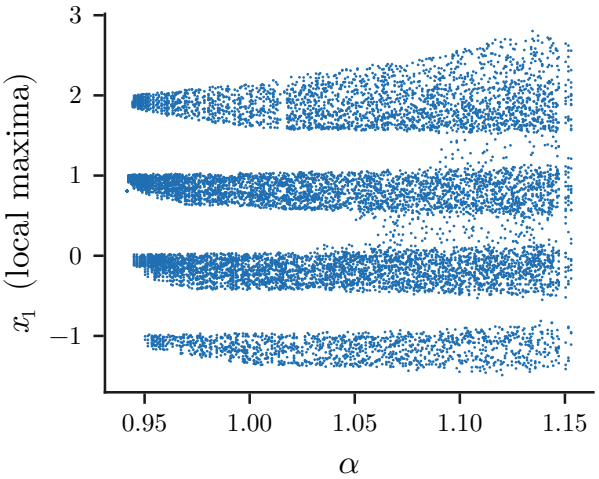


Fig. 9: Bifurcation diagram of the FOUDS-II system (27)–(28): local maxima of x_1 versus the fractional order α.

FOUDS-I example, the valid interval $0 < \alpha < 1.1002$ is limited by the dissipativity condition, while in the FOUDS-II example the window $0.9417 < \alpha < 1.2691$ is limited below by the membership condition and above by the dissipativity condition. In both examples, the bifurcation diagrams indicate irregular dynamics. The FOUDS-II example also shows that the conditions of Definition 2 are not sufficient for the existence of a bounded attractor.

Declarations

Funding. The authors want to thank the Mexican Secretariat of Science, Humanities, Technology and Innovation (SECIHTI) for supporting them with: a master's scholarship for M.A. Mata–González No. 492307; a postdoctoral scholarship for J.R. Pulido–Luna; the *Ciencia Básica y de Frontera* project CBF-2026-2581 and the IIxM program No. 366 for J.A. López–Rentería.

Competing interests. The authors have no competing interests to declare that are relevant to the content of this article.

Ethics approval and consent. Not applicable.

Data availability. All data in this article are produced by numerical simulation with the code described below.

Code availability. The code used in this article is available from the corresponding author on reasonable request.

Author contributions. **M. A. Mata–González**: Formal analysis, Investigation, Software, Writing - original draft. **J. R. Pulido–Luna**: Conceptualization, Funding acquisition, Formal analysis, Software, Writing - original draft, Writing - review &

editing. **J. Álvarez**: Formal analysis, Investigation, Methodology, Writing - review & editing. **J. A. López–Rentería**: Investigation, Conceptualization, Methodology, Funding acquisition, Formal analysis, Supervision, Writing - original draft, Writing - review & editing.

References

[1] Devaney, R.L.: An Introduction to Chaotic Dynamical Systems, 2nd edn. Addison-Wesley, Redwood City, CA, USA (1989)

[2] Wiggins, S.: Introduction to Applied Nonlinear Dynamical Systems and Chaos. Texts Appl. Math., vol. 2. Springer, New York (1990)

[3] Perko, L.: Differential Equations and Dynamical Systems, 3rd edn. Texts in Applied Mathematics. Springer, New York (2001)

[4] Hirsch, M.W., Smale, S., Devaney, R.L.: Differential Equations, Dynamical Systems, and An Introduction to Chaos, 3rd edn. Academic Press, ??? (2013)

[5] Campos-Cantón, E., Barajas-Ramírez, J.G., Solís Perales, G., Femat, R.: Multiscroll attractors by switching systems. Chaos **20**, 013116 (2010) https://doi.org/10.1063/1.3314278

[6] Campos-Cantón, E., Femat, R., Chen, G.: Attractors generated from switching unstable dissipative systems. Chaos **22**(3), 033121 (2012) https://doi.org/10.1063/1.4742338

[7] Campos-Cantón, E., Escalante-González, R.J., Gilardi-Velázquez, H.E.: Generation of Self-Excited, Hidden and Non-Self-Excited Attractors in Piecewise Linear Systems: Some Recent Approaches. World Scientific Publishing, ??? (2023). https://doi.org/10.1142/13347

[8] Aguirre-Hernández, B., Campos-Cantón, E., López-Rentería, J.A., Díaz González, E.C.: A polynomial approach for generating a monoparametric family of chaotic attractors via switched linear systems. Chaos, Solitons & Fractals **71**, 100–106 (2015) https://doi.org/10.1016/j.chaos.2014.12.012

[9] Pulido-Luna, J.R., López-Rentería, J.A., Cazarez-Castro, N.R., Campos-Cantón, E.: A two-directional grid multiscroll hidden attractor based on piecewise linear system and its application in pseudorandom bit generator. Integration **81**, 34–42 (2021) https://doi.org/10.1016/j.vlsi.2021.04.011

[10] Pulido-Luna, J.R., López-Rentería, J.A., Cardenas-Maciel, S.L., Ollervides-Vazquez, E.J., Cazarez-Castro, N.R.: Three-directional multiscroll hidden attractors via piecewise linear systems. In: 2022 International Conference on Mechatronics, Electronics and Automotive Engineering (ICMEAE), Cuernavaca, Mexico, pp. 61–66 (2022). https://doi.org/10.1109/ICMEAE58636.2022.00018

[11] Clemente-López, D., Munoz-Pacheco, J.M., Zambrano-Serrano, E., Félix Beltrán, O.G., Rangel-Magdaleno, J.d.J.: A piecewise linear approach for implementing fractional-order multi-scroll chaotic systems on ARMs and FPGAs. Fractal and Fractional **8**(7), 389 (2024) https://doi.org/10.3390/fractalfract8070389

[12] Caputo, M.: Elasticita e Dissipazione. Zanichelli, Bologna, Italy (1969)

[13] Caputo, M.: Mean fractional-order-derivatives differential equations and filters. Annali dell'Universita di Ferrara **41**, 73–84 (1995)

[14] Matignon, D.: Stability results on fractional differential equations with applications to control processing. In: Proceedings of IMACS-SMC, Lille, France, pp. 963–968 (1996)

[15] Matignon, D.: Stability properties for generalized fractional differential systems. ESAIM: Proceedings **5**, 145–158 (1998) https://doi.org/10.1051/proc:1998004

[16] Podlubny, I.: Fractional Differential Equations. Academic Press, San Diego, CA, USA (1999)

[17] Kilbas, A.A., Srivastava, H.M., Trujillo, J.J.: Theory and Applications of Fractional Differential Equations. Math. Studies, vol. 204. Elsevier (North-Holland), Amsterdam (2006)

[18] Chen, Y., Petras, I., Xue, D.: Fractional order control – a tutorial. In: American Control Conference, St. Louis, MO, USA (2009)

[19] Petras, I.: Stability of fractional-order systems with rational orders: A survey. Fractional Calculus & Applied Analysis **12**(3), 269–298 (2009)

[20] Petras, I.: Fractional-Order Nonlinear Systems: Modeling, Analysis and Simulation. Springer, Berlin, Heidelberg (2011)

[21] Yan, S., Wang, Q., Sun, X., Song, Z.: Multiscroll fractional-order chaotic system and finite-time synchronization. Physica Scripta **97**(2), 025203 (2022) https://doi.org/10.1088/1402-4896/ac4944

[22] Yu, F., Xu, S., Lin, Y., He, T., Wu, C., Lin, H.: Design and analysis of a novel fractional-order system with hidden dynamics, hyperchaotic behavior and multi-scroll attractors. Mathematics **12**(14), 2227 (2024) https://doi.org/10.3390/math12142227

[23] Tlelo-Cuautle, E., Pano-Azucena, A.D., Guillén Fernández, O., Silva-Juárez, A.: Characterization and optimization of fractional-order chaotic systems. In: Analog/Digital Implementation of Fractional Order Chaotic Circuits and Applications. Springer, Cham (2019). https://doi.org/10.1007/978-3-030-31250-3_3

[24] Yao, J., Wang, K., Huang, P., Chen, L., Tenreiro Machado, J.A.: Analysis and

implementation of fractional-order chaotic system with standard components. Journal of Advanced Research **25**, 97–109 (2020) https://doi.org/10.1016/j.jare.2020.05.008

[25] Freeborn, T.J.: A survey of fractional-order circuit models for biology and biomedicine. IEEE Journal on Emerging and Selected Topics in Circuits and Systems **3**(3), 416–424 (2013) https://doi.org/10.1109/JETCAS.2013.2265797

[26] Tavakoli-Kakhki, M., Haeri, M., Saleh Tavazoei, M.: Simple fractional order model structures and their applications in control system design. European Journal of Control **16**(6), 680–694 (2010) https://doi.org/10.3166/ejc.16.680-694

[27] Chen, L., Pan, W., Wang, K., Wu, E., Tenreiro Machado, J.A., Lopes, A.M.: Generation of a family of fractional order hyper-chaotic multi-scroll attractors. Chaos, Solitons & Fractals **105**, 244–255 (2017) https://doi.org/10.1016/j.chaos.2017.10.032

[28] Echenausía-Monroy, J.L., Huerta-Cuellar, G., Jaimes-Reátegui, R., García-López, J.H., Aboites, V., Cassal-Quiroga, B.B., Gilardi-Velázquez, H.E.: Multistability emergence through fractional-order-derivatives in a pwl multi-scroll system. Electronics **9**(6), 880 (2020) https://doi.org/10.3390/electronics9060880

[29] Echenausía-Monroy, J.L., Gilardi-Velázquez, H.E., Wang, N., Jaimes-Reátegui, R., García-López, J.H., Huerta-Cuellar, G.: Multistability route in a pwl multi-scroll system through fractional-order derivatives. Chaos, Solitons & Fractals **161**, 112355 (2022) https://doi.org/10.1016/j.chaos.2022.112355

[30] Ramos-Fabian, C.A., Pulido-Luna, J.R., Cazarez-Castro, N.R., López Rentería, J.A.: Multi-scroll attractors and multi-stability generated via fractional-order switching linear systems. Memorias del Congreso Nacional de Control Automático, 479–484 (2023) https://doi.org/10.58571/CNCA.AMCA.2023.064

[31] Munkres, J.R.: Topology. Prentice-Hall, Massachusetts (2000)

[32] Marsden, J.E., Hoffman, M.J.: Basic Complex Analysis. W. H. Freeman, United Kingdom (1999)

[33] Diethelm, K., Ford, N.J., Freed, A.D.: A predictor-corrector approach for the numerical solution of fractional differential equations. Nonlinear Dynamics **29**, 3–22 (2002)